J. Membrane Biol. 197, 193–202 (2004)
DOI: 10.1007/s00232-004-0653-3

The Journal of
Membrane
Biology

Volume-dependent Glutamate Permeation Depends on Transmembrane Ionic Strength and Extracellular Cl^-

M.M. Hoffman[1], **S.S. Garber**[1,2]
[1]Dept. of Pharmacology and Physiology, College of Medicine, Drexel University, USA
[2]Dept. of Physiology and Biophysics, Finch University of Health Sciences/The Chicago Medical School, North Chicago, IL 60064, USA

Received: 3 September 2003/Revised: 16 December 2003

Abstract. Many mammalian cells regulate their volume by the osmotic movement of water directed by anion and cation flux. Ubiquitous volume-dependent anion currents permit cells to recover volume after swelling in response to a hypotonic environment. This study addressed competition between glutamate (Glu) and Cl^- permeation in volume-activated anion currents in order to provide insight into the ionic requirements for volume regulation, volume-dependent anion channel activity and to the architecture of the channel pore. The effect of changing the intracellular molar fraction (MF) of Glu and Cl^- on conductance and relative anion permeability was evaluated as a function of the extracellular permeant anion and/or the ionic strength. Relative permeability of Glu to Cl^- was determined by measuring reversal potentials under defined ionic conditions. Under conditions with high (150 mM) or low (50 mM) ionic strength solutions on both sides of the membrane, Cl^- was always more permeable than Glu. When a transmembrane ionic strength gradient (150 mM extracellular: 50 mM intracellular) was set to drive water into the cell, and in the presence of extracellular Cl^-, Glu became up to 16-fold more permeable than Cl^-. Replacement of extracellular Cl^- with Glu abolished this effect. These results indicate that it is possible for Glu to move into the extracellular environment during volume-regulatory events and they support the emerging role of glutamate as a modulator of anion channel activity.

Key words: Anion channel — Cell volume regulation — Anomalous mole fraction — Anion permeation

Correspondence to: S.S. Garber; email: garbers@finchcms.edu

Introduction

Most mammalian cells maintain their volume within a narrow range. Maintaining and regulating cell volume via processes as diverse as lymphocyte activation, cell cycle regulation, proliferation, and apoptosis is critical (Garber & Cahalan, 1997; Lang et al., 1998b). Some cells, namely blood cells, cells of the renal medullary interstitium and glia are routinely exposed to dramatic changes in their osmotic environment (Law, 1991). Pathophysiological conditions, such as polydipsia-hyponatremia, encountered in untreated diabetes or chronic schizophrenia, may also lead to osmotic challenges in a variety of cell types (McManus, Churchwell & Strange, 1995; Nilius et al., 1997).

The acute cellular response to swelling involves a rapid efflux of anions and cations, which helps restore volume through a process called regulated volume decrease (RVD). Volume-dependent anion channels, which contribute to RVD, are permeable to such biologically active anions as chloride and glutamate (Glu) (Garber & Cahalan, 1997; Lang et al., 1998a; Levitan & Garber, 1998; Pasantes-Morales et al., 2000). These currents are found in many cell types, including kidney cells and glia (e.g., Lang & Paulmichl, 1995; Emma, McManus & Strange, 1997; Darby et al., 2003).

Glu, unlike other volume-sensitive amino acids such as taurine, is negatively charged at physiological pH. Thus, Glu movement through and interaction with the pore of the volume-dependent anion channels can be followed electrophysiologically. Permeant anions have been suggested to be involved in modulating volume-dependent anion conductances via intra-and/or extracellular anion binding sites, although Glu has not been specifically mentioned (e.g., Stutzin et al., 1997; Stutzin et al., 1998; Doroshenko, 1999). Glu, however, is a biologically active compound. For

example, Glu has been reported to control anion selectivity in the cystic fibrosis transmembrane regulator (CFTR), though the action of Glu appears to be as an intracellular agent rather than via action as a permeant anion (Reddy & Quinton, 2003). The role of Glu in RVD is also of particular interest in the brain because of its neuro-active properties and its role in anxiety, depression, addiction and schizophrenia. Glu is released from astrocytes via activation of volume-dependent anion channels and may contribute to excitotoxic damage (Basarsky, Feighan & MacVicar, 1999).

In this study, we addressed the hypothesis that Glu competes with Cl^- for permeation through a volume-dependent anion current. A human embryonic kidney cell line, tsA201a, was used as a model system in part because the volume-dependent anion channel expressed by this cell is similar to that reported in other systems (e.g., Jackson & Strange, 1995; Lang & Paulmichl, 1995; Garber & Cahalan, 1997). The interaction between Glu and Cl^- within the volume-dependent anion channel was determined by varying the intracellular molar fraction (MF) of the two anions. The contributing role of the transmembrane ionic strength was also determined because cell swelling leads to a transient decrease in intracellular ionic strength and these changes are thought to contribute to activation of volume-dependent anion currents (Emma et al., 1997; Nilius, Eggermont & Droogmans, 2000; Pasantes-Morales et al., 2000).

This study reports that the relative permeability of Cl^- and Glu can be changed dramatically when a transmembrane ionic-strength gradient was set to drive water into the cell. Under these conditions, in the presence of extracellular Cl^-, Glu became much more permeable than Cl^-, indicating that it is possible for Glu to move into the extracellular environment during volume regulatory events. These data support the emerging role of Glu as a modulator of anion channel activity.

Materials and Methods

Cell Culture

tsA201a cells were grown and maintained in Dulbecco's Modified Eagle's Medium (DMEM) supplemented with 10% fetal bovine serum (FBS) and 100 units penicillin and 100 μg streptomycin per ml of medium (DMEM complete) at 37°C at 5% CO_2 (Margolskee, McHendry-Rinde & Horn, 1993). Cells were plated 12–16 hours prior to an experiment onto polylysine coated coverslips. Only one cover slip was used at a time and was rinsed with the external recording solution prior to being placed in the recording dish.

Whole-Cell Recording

Macroscopic ionic currents were measured using the whole cell-recording configuration of the standard patch-clamp technique (Hamill et al., 1981). Pipettes were pulled from 7052 glass (Garner Glass, Claremont, CA) using a glass microelectrode puller, coated with Sylgard® 184 (Dow Corning, Midland, MI), and fire-polished to give a final resistance of 4–10 MΩ in the recording solutions. Currents were recorded using an EPC9 amplifier (HEKA Electronik, Lambrecht, Germany) and the accompanying acquisition and analysis software. Further analysis employed IGOR (WaveMetrics, Lake Oswego, OR) and Microsoft EXCEL (Microsoft, Redmond, VA). Net junction potential was nulled immediately before seal formation. Pipette and whole cell capacitance were automatically compensated and recorded. Whole cell capacitance and series resistance (R_s) were monitored throughout the recording. Series resistance compensation was employed at 45 to 95% compensation with a 100 μs lag. Errors in the measurement of the reversal potential as a result of series resistance error are negligible. Normal cellular current convention is used when referring to the direction of current. All experiments were performed at room temperature (22°C ± 2). Exchange of the intracellular solution (as indicated by the washout of cation currents) into the cell occurred within 30 s after whole-cell configuration was established.

Table 1. Composition of extracellular solutions at high and low ionic strength (IS)

	Cl^- high IS*	Cl^- low IS	Glu high IS
Cl	150	50	0
Glu	0	0	150
EGTA	1	1	1
$CaCl_2$	2	2	2
HEPES	10	10	10

Concentrations are given in mM. Solutions were adjusted to pH 7.2 with 1M HCl or NMDG. Osmolality was adjusted with sucrose to 313 or 250 ± 5 mOsm, as experimentally dictated. *IS = ionic strength.

Recording Solutions

Anion current was isolated using pipette and bath solutions that contain N-methyl, D-Glucamine (NMDG-OH), a large impermeant cation as a counter ion rather than Na^+ or K^+, to prevent cation currents. The ionic composition of extracellular recording solutions is given in Table 1. The ionic composition of the intracellular pipette solutions is shown in Table 2. Cl^- solutions were made using HCl to obtain the indicated [Cl^-]. Glutamic acid was used to obtain the indicated [Glu]. The pH of all solutions was adjusted with NMDG to 7.2. Although ATP hydrolysis is not required, 4 mM ATP is required in intracellular solutions in order to maintain recordings of the volume-regulated anion current (Cahalan & Lewis, 1988; Lewis, Ross & Cahalan, 1993; Ross, Garber & Cahalan, 1994). Solutions containing molar fractions (MF = [Glu]/{[Glu] + [Cl^-]}) of Glu and Cl^- ranging from MF = 0.0 to 1.0 were achieved by mixing solutions containing the individual anions. A small [Cl^-] (0.2 mM) was always present in Glu solutions to allow for electrode stability.

It is possible that more than one anion channel is activated under these experimental conditions. Nanomolar (nM) levels of intracellular [Ca^{++}] were maintained with EGTA to prevent activation of Ca^{2+}-dependent current (Garber, Hoshi & Aldrich, 1989). The experimental conditions rule out Ca^{2+}-activated anion conductance. CIC-3, which has been suggested to have a role in volume regulation (Hume et al., 2000; Li & Weinman, 2002), is expressed in tsA201a cells at a low level, and its activation is unlikely in the absence of exogenous CAM Kinase II (Huang et al., 2001; *see* also Maduke, Miller & Mindell, 2000; and Jentsch et al.,

Table 2. Molar fraction (*MF*) of Glu and Cl^- in intracellular solutions

	Low IS*		High IS	
MF^	[Cl] (mm)	[Glu] (mm)	[Cl] (mm)	[Glu] (mm)
0	50	0	150	0
0.1	45	5	135	15
0.2	40	10	120	30
0.5	25	25	75	75
0.8	10	40	30	120
0.9	5	45	15	135
1.0	0.2#	50	0.2#	150

Solutions also contain (in mM): 1.1 EGTA, 0.1 $CaCl_2$, 10 HEPES, 4 ATP, pH 7.2. NMDG was the cation in all solutions. Osmolality was adjusted to 313 ± 5 mOsm with sucrose. *IS = ionic strength. ^*MF* indicates intracellular molar fraction of Cl^- and Glu ([Glu]/([Cl] + [Glu]). #[Cl] to allow for Ag/AgCl electrode stability.

2002, for reviews of the physiological roles of CIC channels.) It is possible that a Ca^{2+}-independent form of CIC-3, or another chloride channel, is expressed. There was no evidence of expression of CFTR or a CFTR-like current in tsA201a cells, and, in any event, experimental conditions preclude its activation.

Transmembrane Osmotic Gradient and Solution Osmolality

An osmotic gradient, required to activate the anion current, was generated when a whole-cell recording configuration was formed, using a pipette solution 35–75 mOsm greater than that of the bath solution. A transmembrane hypotonic gradient was formed using either 330 ± 5 mOsm, inside, and 295 ± 5 mOsm, outside, or 375 ± 5 mOsm, inside, and 295 ± 5 mOsm outside. Current activation was dependent on the transmembrane osmotic gradient, but independent of the magnitude of the hypotonic gradient. Recordings made with higher intracellular osmolality tended to last longer than those made with lower intracellular osmolality. Extracellular isotonic osmolality in which cells maintained original volume for tsA201a cells was determined to be 313 ± 3 mOsm.

Solution osmolarity was adjusted by addition of sucrose or glucose to the required osmolality. For example, isotonic extracellular solutions of high ionic strength contained very little sucrose (1–5 mM), whereas low ionic strength solutions contained 200–210 mM sucrose in order to obtain a final solution osmolality of 310–315 mOsm. Extracellular hypotonic solutions were similarly adjusted. Intracellular solutions were adjusted to an isotonic osmolality of 310–315 mOsm or a hypertonic osmolality of 370–380 mOsm with either sucrose or glucose. Measured reversal potentials were indifferent to osmotic adjustments made with either glucose or sucrose.

The osmolality of all solutions was determined immediately before experiments with a vapor pressure osmometer (Wescor, Logan, Utah). Final adjustments in solution osmolality were made with the addition of 1–10 μl water (decreasing osmolality) or 1–5 mM sucrose or glucose (increasing osmolality). Care was taken to ensure the ionic composition, and strength of the solutions was as experimentally dictated. Ionic composition and strength were maintained irrespective of osmotic gradient.

Ionic Strength

Ionic strength (Γ) may be calculated using the Debye-Huckel-Limiting Law:

$$\Gamma = 0.5\Sigma c_i z_i^2 \quad (1)$$

where c_i, is concentration and z_i is the charge of the i^{th} ionic species (Smith & Miller, 1985). Ideally ionic activity (a) should be used to calculate ionic strength since at high ionic strength $a < c_i$ (Hamill et al., 1981). The value of 'a' is not readily available for all ions, therefore 'c' was used in accordance to common practice in the literature (Nilius et al., 1998; Smith & Miller, 1985). An additional complication for calculating absolute ionic strength of solutions is that apparent affinity of EGTA for Ca^{2+} is dependent on pH, temperature and ionic strength. A small portion of HEPES will also be anionic at pH 7.2. In order to reduce the contribution of these complications to calculations of ionic strength, the difference in (not absolute) ionic strength between solutions will be considered. In addition, the contributions of EGTA, Ca^{2+} and HEPES will be assumed to be negligible compared to an ionic strength difference of 150 mM NMDG-Cl and 50 mM NMDG-Cl. For this example, $\Delta\Gamma = 100$ mM $= 0.5\{[Cl^-]_{out}(-1)^2 - [Cl^-]_{in}(-1)^2 + [NMDG^+]_{out}(1)^2 - [NMDG^+]_{in}(1)^2\}$. High ionic strength solutions contain either 150 mM Cl^- or Glu and low ionic strength solutions contained an anion mixture ranging from 50 mM Cl^- to 50 mM Glu.

Analysis

Current amplitude increased over time and reached a maximum level under all experimental conditions tested. In some cases, the current amplitude declined after reaching a peak value. The initial rate of current activation was calculated from the initial linear portion of the increasing current amplitude over time (experiments ranged from 5–20 min in duration). The average current under each ionic condition was determined after subtraction of the initial leak current measured at time $t = 0$. Reversal potentials were determined directly from current traces and corrected for liquid junction potentials calculated using JPCalc, Junction Potential Software developed by Dr. P.H. Barry (Cell MicroControls, Virginia Beach, VA). Table 3 shows the values of these calculations for the solutions tested. Ion concentrations were determined after pH titration. Uncertainties in measuring and titration resulted in some variation (< 5%) between batches of solutions. Junction potential calculations were made for each specific solution used for an individual measurement. Permeability ratios were calculated from measured reversal potentials using a standard form of the Goldman-Hodgkin-Katz equation, rearranged to solve for the permeability ratio (where 'A-' is an anion).

$$P_{A^-}/P_{Cl} = \frac{e^{v_r(zF/RT)}[Cl]_{out} - [Cl]_{in}}{[A^-]_{in} - e^{v_r(zF/RT)}[A^-]_{out}} \quad (2)$$

Averages are presented as ± standard error of the mean. Significance was determined using an unpaired Student's t-test where $P < 0.01$. Measurements were made from over 140 cells.

Results

Symmetrical Ionic Strength

Figure 1 shows examples of families of currents recorded with either low ionic strength or high ionic strength on both sides of the membrane. Currents were activated with an 80% (outside/inside osmolality) transmembrane osmolality gradient. Current inactivation was not appreciable within the voltage range (−60 to +120 mV) tested. The molar fraction

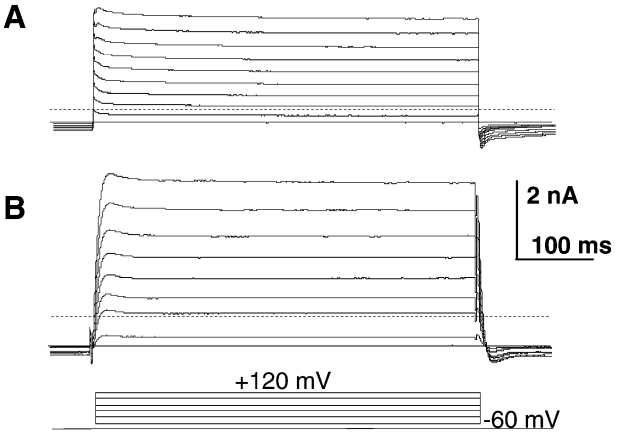

Fig. 1. Families of current responses in tsA201a cells are shown in response to a 500 ms voltage pulse from a holding potential of −60 mV to 120 mV. Protocol is shown schematically below current traces. (*A*) An example of a volume-regulated anion current recorded in internal and external solutions of low ionic strength, *MF* = 0.8. (*B*) An example of a volume-regulated anion current recorded in internal and external solutions of high ionic strength, *MF* = 0.0. Dashed line represents zero current. Current traces have not been modified. Transmembrane osmotic (outside/inside) gradient, $\Delta\Pi$ = 0.80, was the same in *A* and *B*.

of Cl^- and Glu had no effect on the time dependence of the current in response to a voltage stimulus from −60 to +160 mV is similar in the current families shown in Fig. 1*A* and 1*B*. These examples were recorded with an intracellular *MF* = 0.8 (symmetrical low ionic strength) or *MF* = 0.0 (symmetrical high ionic strength), respectively. Current families and time dependence of currents was similar under all other conditions.

The amplitude of the volume-regulated anion conductance increased over time in response to a hyposmotic transmembrane gradient. An example comparing the increase of the current amplitude at +60 mV over time in recordings made in symmetrical high or low ionic strength with an intracellular *MF* = 0.5 is shown in Fig. 2*A*. The initial increase in current amplitude occurred at the same rate, independent of the ionic strength of the recording solution.

Previous work has shown that the initial rate of increase of the current amplitude corresponds to the activation of this current in response to cell swelling under whole-cell conditions (Levitan & Garber, 1997). Figure 2*B* shows that with high ionic strength solutions on both sides of the membrane, the initial slope does not vary with intracellular MF. The initial slope under symmetrical low ionic strength conditions and an intracellular *MF* = 0.2 is significantly greater ($P < 0.04$) than that at *MF*s = 0.1, 0.5 and 0.8 or *MF* = 0.2 under symmetrical high ionic strength solutions. Thus the data in Fig. 2 indicate that the combination of ionic strength and the intracellular *MF* of Cl^- and Glu had an effect on current activation and the rate of water entering the cell during swelling.

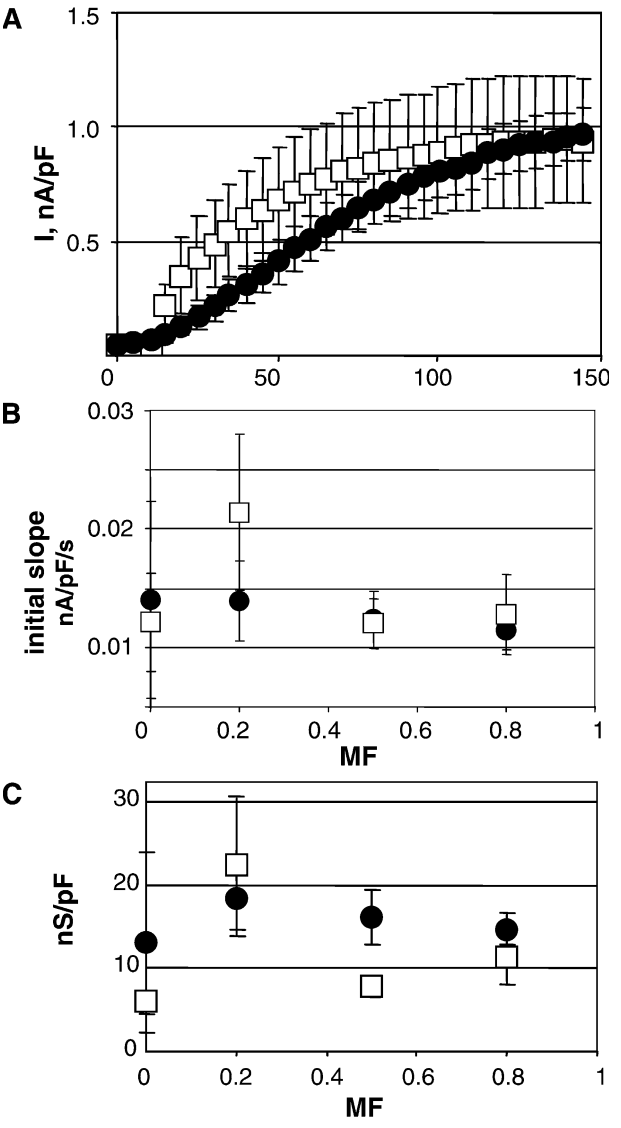

Fig. 2. Development of volume-dependent anion current over time. (*A*) Current at 60 mV was recorded from the initiation of the whole-cell recording configuration, with ionic strength solutions that are both high (●) or low (□) on both sides of the membrane. Current amplitudes were corrected for leak current recorded at *t* = 0 and averaged. *MF* of pipette solution was 0.5. (*B*) Initial slope of anion current activation varies with intracellular *MF* in symmetrical low (□) but not high (●) ionic strength solutions. (*C*) Maximal conductance varies with intracellular *MF*. Measurements made in high (●) and low (□) ionic strength solutions are shown, $n \geq 5$, ± SEM and $\Delta\Pi$ = 0.80 under all conditions.

The amplitude of the volume-dependent anion current reached a steady plateau after 100–200 s under most conditions. In order to determine the potential contribution of this current to RVD over a longer period, the effect of ionic strength and intracellular *MF* on anion conductance was determined 300 s after current activation. Figure 2*C* shows the anion conductance per unit membrane at molar fractions from = 0.0 to 0.8, in either low or high

ionic strength symmetrical recording solutions. The conductance is similar, regardless of ionic strength, suggesting that a similar amount of current is flowing under each condition. The conductance at 300 s peaked at $MF = 0.2$ under each ionic strength condition, although the increase in conductance at $MF = 0.2$ under symmetrical low ionic strength conditions was significant ($P < 0.04$) with respect to $MF = 0$, 0.5 and 0.8. This was not the case under symmetrical high ionic strength conditions.

Transmembrane Ionic Strength Gradient

Intracellular ionic strength decreases as water enters a cell during swelling. It was, therefore, of interest to determine the effect on current amplitude of a transmembrane ionic strength gradient, as an increase in current suggests that the current will play a greater role in RVD. We also compared the effect of the extracellular anion on current amplitude.

In the presence of a transmembrane ionic gradient, the amplitude of the volume-dependent anion conductance increased over time (Fig. 3*A*) in a manner similar to that in the absence of such a gradient (Fig. 2*A*). The initial rate of increase in current amplitude, however, depended on both the extracellular anion and the intracellular *MF* (Fig. 3*B*). The rate was greater in the presence of extracellular Cl^- ($P < 0.06$ when $MF = 0.1$; $P < 0.002$ when $MF = 0.5$). The rate in the presence of a transmembrane ionic strength gradient and extracellular Cl^- was also greater than under symmetrical high or low ionic strength conditions (*compare* Figs. 2*B* and 3*B*; $P < 0.003$ at $MF = 0.5$).

In the presence of a transmembrane ionic strength gradient and extracellular Glu, the initial rate was at least 2-fold lower when $MF = 0.1$ and decreased significantly ($P < 0.05$) with an increasing fraction of Glu in the intracellular solution. The rate in the presence of a transmembrane ionic strength gradient and extracellular Glu was also significantly less than under symmetrical high or low ionic strength conditions (*compare* Figs. 2*B* and 3*B*; $P < 0.02$ at $MF = 0.02$ and 0.5). Anion conductance at 300 s also decreased ($P < 0.02$ at $MF = 0.05$) in the presence of extracellular Glu (Fig. 3*C*).

Thus, current amplitude is greatest in the presence of a transmembrane ionic strength gradient and extracellular Cl^-. The experimental ionic conditions used here approximate those expected during cell swelling.

Anion Permeability Depends on Ionic Conditions

Anion movement across the plasma membrane is an integral component to cellular volume regulation. Both Cl^- and Glu may be used as osmolytes in addition to being biologically active anions. In order to determine which anion, Cl^- or Glu, is more likely to permeate the volume-dependent anion channel, and thereby contribute to RVD, we determined the relative permeability of the two anions under conditions in which they were competing for occupancy of the channel.

The relative permeability of Cl^- and Glu was determined by measuring the shift of reversal

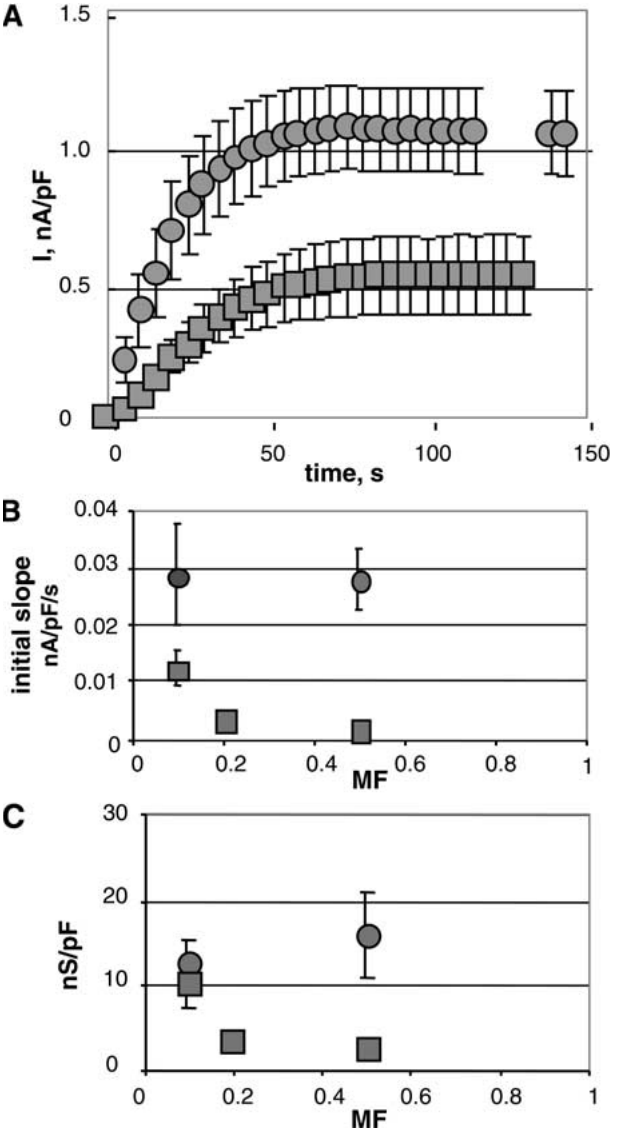

Fig. 3. Development of volume-dependent anion current in response to transmembrane ionic strength gradient ($\Delta\Gamma = 100$) depends on extracellular anion. (*A*) Current at 60 mV was recorded from the initiation ($t = 0$) of the whole-cell recording configuration. Extracellular solutions contained Cl^- (●) or Glu (■). *MF* of pipette solution was 0.1. Current amplitudes were corrected for leak current recorded at $t = 0$ and averaged. (*B*) Initial slope of anion current with extracellular solutions containing Cl^- (●) or Glu (■) varies with intracellular *MF*. (*C*) Maximal conductance varies with intracellular *MF* when extracellular solutions contained Cl^- (●) or Glu (■). Transmembrane ionic strength gradient, $\Delta\Gamma = 100$, $\Delta\Pi = 0.80$ and ($n \geq 5$, ± SEM) under all conditions.

potentials (V_r) as a function of the molar fraction of these two anions. Currents were elicited by a voltage ramp from −60 to +100 mV. Examples of I/V traces shown in Fig. 4*A* and 4*B* were recorded in low or high ionic strength recording solutions, respectively. Reversal potentials, shown in Table 4, were measured when the maximal current amplitude had stabilized. The shape of the current-voltage relationships was similar under all recording conditions, although the amplitude of the examples shown varies, as traces shown have not been normalized for cell capacitance. Permeability ratios (P_{Glu}/P_{Cl}) were calculated from the measured reversal potential shifts (Tables 4) after correction for liquid junction potentials (Table 3).

Figure 4*C* shows that, in symmetrical high or low ionic strength solutions, the permeability of Glu was always less than that of Cl^- (i.e., $P_{Glu}/P_{Cl} < 1.0$). The relative permeability of Cl^- and Glu, however, varied as the intracellular molar fraction of Glu moved from 0 toward 1.0. In symmetrical high ionic strength solutions P_{Glu}/P_{Cl} was significantly different ($P < 0.005$) at $MF = 0.5$ and 0.8. In symmetrical low ionic strength solutions P_{Glu}/P_{Cl} was significantly different ($P < 0.05$) at $MF = 0.2$, 0.5 and 0.8. Variation of P_{Glu}/P_{Cl} with MF indicates more than one anion binding site and the anions interact within the pore (Hille, 1992).

The relative permeability of Cl^- and Glu changed dramatically when measured in the presence of a transmembrane ionic strength gradient. Examples of currents elicited under these conditions by a voltage ramp from −60 to +100 mV are shown in Figs. 5*A* and 5*B*. Reversal potentials are tabulated in Table 4.

P_{Glu}/P_{Cl} showed a strong dependence on the intracellular anion composition in the presence of extracellular Cl^- and a transmembrane ionic strength gradient (Fig. 5*C*). In the presence of extracellular Cl^- P_{Glu}/P_{Cl} was greater than 1.0 for all *MF*s tested. Glu became more permeable than Cl^- under these conditions, with P_{Glu}/P_{Cl} ranging from 16 to 3 as the intracellular MF was varied from 0.1 to 0.9. In contrast, P_{Glu}/P_{Cl} was less than 1.0 for all *MF*s tested in the presence of extracellular Glu. Thus the relative permeability of Glu and Cl^- depended on the extracellular anion and a transmembrane ionic strength gradient.

A concern was that an excitatory amino-acid transporter (EAAT) was activated when cells were exposed to extracellular high ionic strength, Cl^--containing solution and low ionic strength intracellular solution. Therefore, reversal potentials were measured in the presence of 10 μM L-(−)-threo-3-hydroxyaspoartic acid (L-THA). L-THA acts as an alternative substrate at EAAT1-4 and as a non-transportable substrate at EAAT5 (Arriza et al., 1994, 1997; Fairman et al., 1995; Lin et al., 1998). Addition of 10 μM L-THA to both the intra- and extracellular solutions did not change the measured

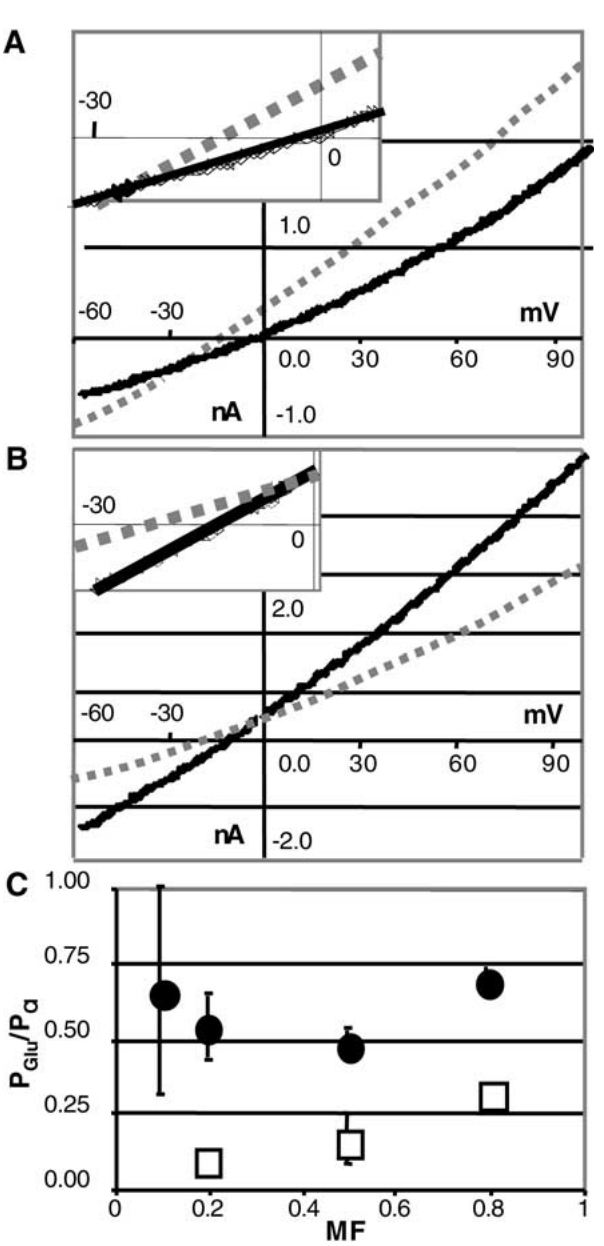

Fig. 4. P_{GLU}/P_{CL} Varies with intracellular MF when ionic strength is the same on both sides of the membrane. Representative raw current traces are shown for solutions with either high (*solid line*) or low (*broken line*) ionic strength on both sides of the membrane. Current was elicited in response to a 500 ms voltage ramp from −60 to 100 mV after activation at $t = 0$. (*A*) $V_t = -5.8 \pm 0.1$ mV in symmetrical high ionic strength solutions (*solid black line*) or $V_r = -15.6 \pm 0.1$ in low ionic strength symmetrical solutions (*broken gray line*) when intracellular $MF = 0.2$. (*B*) When intracellular $MF = 0.5$, $V_r = -16.7 \pm 0.1$ mV with high ionic strength symmetrical solutions (*solid black line*) and $V_r = -20.9 \pm 0.1$ mV with low ionic strength symmetrical solutions (*broken gray line*). Insets in *A* and *B* show detail of area near V_r. Solid black or gray lines superimposed on data point indicate linear fit to data used to determine V_r. (*C*) Cl^- is more permeant that Glu, but P_{Glu}/P_{Cl} varies with intracellular MF when determined in solutions with either high (●) or low (□) ionic strength on both sides of the membrane ($n = 5$, ± SEM). $\Delta\Pi = 0.80$ under all conditions.

Table 3. Liquid junction potentials

MF^	OUT IN	Cl^- high IS* hypo high IS	Cl^- low IS hypo low IS	Cl^- high IS hypo low IS	Glu high IS hypo low IS
0		−0.2	−0.6		
0.1		1.2		15.3	−8.6
0.2		2.8	2.2	16.5	−7.1
0.5		8	7.1	20.4	−4.9
0.8		14.6	13.3	25.2	
0.9				27.2	

Junction potentials were calculated using JPCalc (Cell MicroControls, Virginia Beach, VA). Composition of solutions is provided in Tables 1 and 2. Extracellular anion, ionic strength and osmotic gradients are indicated in row labeled "OUT". Intracellular ionic strength is indicated in row labeled "IN". *IS = ionic strength. ^*MF* indicates intracellular molar fraction of Cl^- and Glu ([Glu]/([Cl] + [Glu]).

Table 4. Measured reversal potentials (uncorrected)

MF^	OUT IN	Cl^- high IS* hypo high IS	Cl^- low IS hypo low IS	Cl^- high IS hypo low IS	Glu high IS hypo low IS	Cl^- high IS iso low IS	Glu high IS iso low IS
0		−2 ± 2 (3)	−11 ± 3 (7)				
0.1		−6 ± 1 (6)		−22 ± 1 (13)	8 ± 3 (7)	−17 ± 2 (6)	6 ± 2 (7)
0.2		−6 ± 1 (11)	−15 ± 2 (6)	−21 ± 1 (5)	6 ± 2 (5)		
0.5		−17 ± 1 (7)	−22 ± 2 (6)	−31 ± 2 (12)	0.1 ± 2 (5)		
0.8		−22 ± 1 (11)	−31 ± 1 (7)	−28 ± 3 (11)			
0.9				−27 ± 2 (10)			

Intracellular molar fraction (*MF*) of Glu and Cl^-, is indicated. Composition of solutions is provided in Tables 1 and 2. Extracellular anion, ionic strength and osmotic gradients are indicated in row labeled "OUT". Intracellular ionic strength is indicated in row labeled "IN". *IS = ionic strength. ^*MF* indicates intracellular molar fraction of Cl^- and Glu^- ([Glu]/([Cl] + [Glu]). SEM and number of experiments/condition (*n*) are indicated.

reversal potential at intracellular $MF = 0.2$ when compared to that measured in matched control cells ($V_r = -21 \pm 4$ mV ($n = 6$) and -19 ± 5 mV($n = 7$), L-THA and control, respectively).

Discussion

These results provide insight into the ionic requirements for volume regulation, volume-dependent anion channel activity and into the architecture of the channel pore. First, a transmembrane ionic strength gradient, not just low intracellular ionic strength is critical to anion movement through the volume-dependent anion channel. Secondly, both intracellular and extracellular anion composition are important. Glu has two major effects on volume-dependent anion channel activity: One as a permeant anion that interacts with Cl^- within the channel pore, and two as an extracellular anion contributing to the regulation of anion permeability.

Several earlier studies have indicated the importance of ionic strength in volume-regulated anion current activity (Jackson et al., 1996; Emma et al., 1997; Cannon, Basavappa & Strange, 1998; Nilius et al., 1998; Voets et al., 1999). This study is distinct in using a large non-permeant cation, $NMDG^+$, as the cationic counter ion rather than Na^+ or Cs^+. Cannon et al. (1998) and Jackson et al. (1996) have observed an increase in the relative cation permeability of this current with a reduction in the intracellular ionic strength. By using $NMDG^+$, we were able to interpret changes in relative anion permeability that may have been masked by increased cation permeability under experimental conditions. Differences between results reported in this study and those of previous studies may be explained by this choice of a non-permeant cationic counter ion. For example, Cannon, et al. (1998) reported that current activation under symmetrical low ionic conditions was greater than that in symmetrical high ionic conditions, whereas we report that current activation is similar. This can be explained by an increase in cation permeability in the presence of Na^+ and Cs^+ that is not observed with $NMDG^+$.

Differences in the number of activated single channels and/or single channel conductance could account for differences observed in the anion conductance per unit membrane under symmetrical ionic strength conditions. Unfortunately, recordings of consistently identifiable single channel activity under parallel ionic conditions, such as those described by (Sabirov et al., 2000), were difficult to obtain with extended effort. The whole-cell data do suggest, however, that given a driving force, a similar amount of anion current moved across the membrane under symmetrical ionic strength conditions, regardless of the underlying mechanism. In contrast, the amount

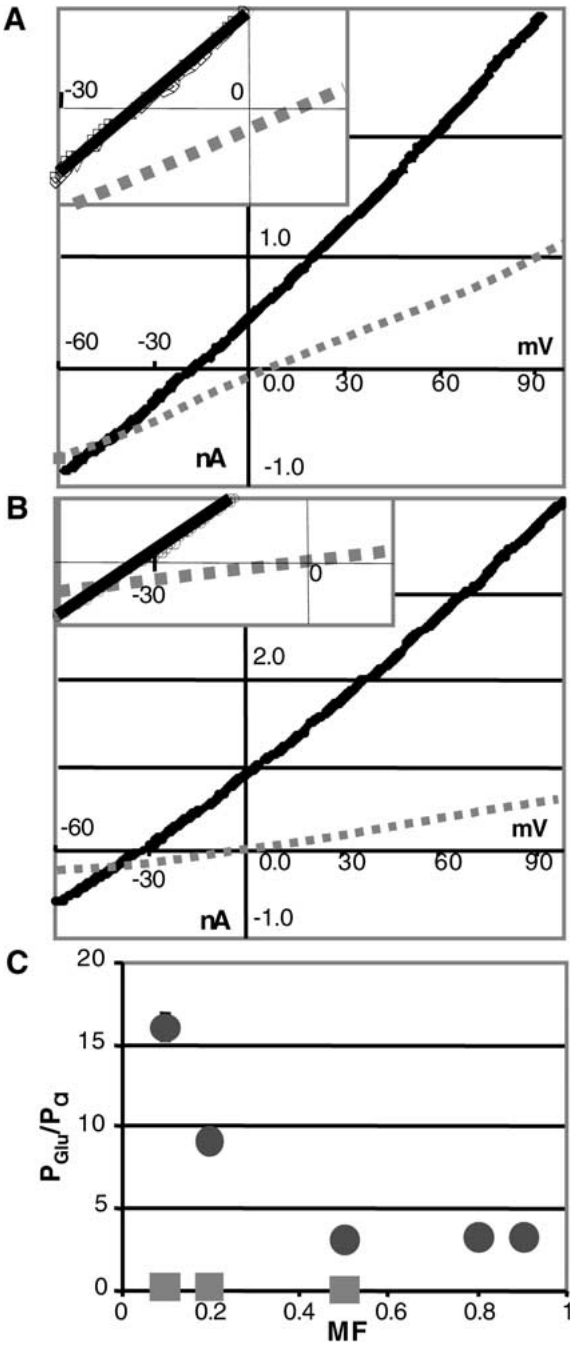

Fig. 5. Glu is more permeable than Cl^- with $\Delta\Gamma = 100$ and Cl^- containing extracellular solutions. Representative raw current traces are shown when extracellular solutions contain either Cl^- (*solid black line*) or Glu (*broken gray line*) and $\Delta\Gamma = 100$. Current was elicited in response to a 500 ms voltage ramp from −60 to 100 mV after activation at $t = 0$. (*A*) With an intracellular $MF = 0.1$, $V_r = -22.5 \pm 0.1$ mV in extracellular Cl^- (*solid black line*) and $V_r = 7.5 \pm 0.1$ in extracellular Glu (—). B. $V_r = -34.7 \pm 0.1$ mV in extracellular Cl^- (*broken gray line*) and $V_r = -0.17 \pm 0.1$ mV in extracellular Glu (*solid black line*) when intracellular $MF = 0.5$. Insets in *A* and *B* show detail of area near V_r. Solid black or gray lines superimposed on data points indicate linear fit to data used to determine V_r.(*C*) Experiments with extracellular Cl^- are shown as (●) or with Glu as (■). Intracellular *MF* was varied as indicated ($n \geq 5$, ± SEM). $\Delta\Gamma = 100$ and $\Delta\Pi = 0.80$ under all conditions.

of anion current that moved in response to a given driving force was highly dependent on the presence of a transmembrane ionic strength gradient.

Ionic Strength and Anion-Dependent Transport Pathway

Our results are consistent with an ion-conductive pathway that can be occupied by more than one permeant species at a time with interactions between the anions possible in the pore. This pathway must be sensitive to the presence of extracellular Cl^-, a transmembrane ionic strength gradient, and intracellular anion composition. This suggests that there are both extra- and intracellular regulatory sites on the volume-regulated channel. These sites appear to be outside of the voltage field across the membrane, as ionic composition has little effect on the shape of the current-voltage relationships under the different conditions.

Contamination by cation currents is unlikely, as the large cation, NMDG, was used in both extra- and intracellular recording solutions. A possible alternative interpretation for our results is that extracellular Cl^-, a transmembrane ionic strength gradient, and the intracellular anion result in activation of a Glu transport pathway that is distinct from the volume-dependent anion conductance. For this to be the case, the transport pathway would be expected to be functionally linked to the volume-regulated channel and have a sufficiently high turnover such that a Glu current contributes to the measured anion current. The transport profile of this protein would need to be such that transport rates are greater with lower $[Glu]_{in}$ and decrease with increased $[Glu]_{in}$. Experiments with the EAAT inhibitor, L-THA, indicate that EAAT1–5 were not involved. Until we can gather data that definitively suggest the identity of a novel Glu transporter, we prefer the interpretation that these ionic effects alter the activity of a volume-dependent anion channel.

Interaction within the Transport Pathway

The unusual dependence of P_{Glu}/P_{Cl} on the intracellular *MF* suggests that the two anions interact within the transport pathway of the volume-dependent anion conductance. Anomalous mole fraction behavior has been reported for a variety of anion channels, including volume-dependent anion currents in lymphocytes, CIC-0 channels, Ca^{2+}-activated Cl channels, neuronal chloride currents and the cystic fibrosis transmembrane-conductance regulator (Franciolini & Nonner, 1994; Fahlke, Durr & George, 1997; Linsdell, Tabcharani & Hanrahan, 1997; Levitan & Garber, 1998; Fahlke, 2000; Qu & Hartzell, 2000). The permeation of Glu through this

volume-dependent anion conductance lends further support to the permeation of other amino acids, which has been observed in many other systems (for review *see* Lang et al., 1998a; Nilius et al., 1997; Pasantes-Morales et al., 2000). Glu was used in this study because it is charged at physiological pH, which allows us to follow currents generated by Glu movement.

Taurine, another amino acid that appears to be involved in volume regulation, is mostly uncharged at physiological pH. Volume-dependent taurine flux may be via an ion channel or an alternate pathway (Huxtable, 1992; Jackson & Strange, 1993; Song, O'Regan & Phillis, 1998; Stutzin et al., 1999; Hussy et al., 2000; Pasantes-Morales et al., 2000). If taurine is permeable through this volume-regulated anion channel, it is likely to appear as a blocker of anion conductance. Impermeant channel blockers do not have any effect on measured reversal potentials, but an electrically silent, permeant molecule that interacts with a charged permeant ion within the channel lumen may alter permeation and may therefore show an anomalous permeation profile.

Implications for Volume Regulation

Water enters a cell during swelling. Recovery requires that water leave the cell in a regulated manner so that the cell may return to its original volume. The regulated movement of anions and cations pulls water from the cell, allowing cell volume recovery. One pathway critical to anion movement is the volume-regulated anion current. This study indicates that anion conductance through this pathway is greatest in the presence of extracellular Cl^-. This result leads to the prediction that regulatory volume decrease observed in intact cells should be more effective in solutions containing Cl^- as the primary anion, as is the case for extracellular solutions found in situ.

The combined effect of an ionic strength gradient and extracellular Cl^- results in a switch in the relative permeability from Cl^- to Glu. While the magnitude of the relative change in permeability is impressive, the magnitude is less important than the apparent change in relative ion permeability. The change in permeability suggests that with a change of intracellular composition in response to swelling, the selectivity mechanism of the channel underlying the volume-dependent anion conductance is altered such that Glu may pass more easily than Cl^- through the ion channel. Osmotically, however, Glu should have the same effect on pulling water out of a swollen cell as Cl^- does.

This change in anion permeability is lost when extracellular solutions contain Glu. In these solutions, Cl^- is always more permeable than Glu. Together, these data suggest that there may be two sites that are important to the regulation of permeation: An external site that is sensitive to the presence of Cl^- (or equivalently, by Glu blocking conduction) and an internal site that is sensitive to ionic strength. Both sites must work together to allow anion permeation. Relative anion permeability of the ion pathway across the membrane would be determined by the relative affinities of these sites to anions under various ionic conditions.

An increased permeability to Glu under swelling conditions has potential physiologically relevant implications, particularly for cells with active Glu uptake or Glu receptors such as glia (Danbolt, 2001). The release of Glu in response to cell swelling in brain tissue might result in the activation of Glu receptors and downstream effects, such as toxicity and/or death (Zipfel et al., 2000). Future experiments will address volume-dependent Cl^-/Glu permeability under more physiological conditions.

We thank Ms. Elizbieta Indyk for excellent technical assistance and Drs. J. Tanaka and H. Rasgado-Flores for excellent suggestions and critical reading of the manuscript. NIDDK46672 and AHA94002340 supported this work.

References

Arriza, J.L., Eliasof, S., Kavanaugh, M.P., Amara, S.G. 1997. Excitatory amino acid transporter 5, a retinal glutamate transporter coupled to a chloride conductance. *Proc. Natl. Acad. Sci. USA* **94:**4155–4160

Arriza, J.L., Fairman, W.A., Wadiche, J.I., Murdoch, G.H., Kavanaugh, M.P., Amara, S.G. 1994. Functional comparisons of three glutamate transporter subtypes cloned from human motor cortex. *J. Neurosci.* **14:**5559–5569

Basarsky, T.A., Feighan, D., MacVicar, B.A. 1999. Glutamate release through volume-activated channels during spreading depression. *J. Neurosci.* **19:**6439–6445

Cahalan, M.D., Lewis, R.S. 1988. Role of potassium and chloride channels in volume regulation by T lymphocytes. *In*: Cell Physiology of Blood. pp. 281–301. Rockefeller University Press, New York

Cannon, C.L., Basavappa, S., Strange, K. 1998. Intracellular ionic strength regulates the volume sensitivity of a swelling-activated anion channel. *Am. J. Physiol.* **275:**C416–C422

Danbolt, N.C. 2001. Glutamate uptake. *Prog. Neurobiol.* **65:**1–105

Darby, M., Kuzmiski, J.B., Panenka, W., Feighan, D., MacVicar, B.A. 2003. ATP released from astrocytes during swelling activates chloride channels. *J. Neurophysiol.* **89:**1870–1877

Doroshenko, P. 1999. High intracellular chloride delays the activation of the volume-sensitive chloride conductance in mouse L-fibroblasts. *J. Physiol.* **514:**437–446

Emma, F., McManus, M., Strange, K. 1997. Intracellular electrolytes regulate the volume set point of the organic osmolyte/anion channel VSOAC. *Am. J. Physiol.* **272:**C1766–C1775

Fahlke, C. 2000. Molecular mechanisms of ion conduction in CIC-type chloride channels: lessons from disease-causing mutations. *Kidney Int.* **57:**780–786

Fahlke, C., Durr, C., George, A.L., Jr. 1997. Mechanism of ion permeation in skeletal muscle chloride channels. *J. Gen. Physiol.* **110:**551–564

Fairman, W.A., Vandenberg, R.J., Arriza, J.L., Kavanaugh, M.P., Amara, S.G. 1995. An excitatory amino-acid transporter with properties of a ligand-gated chloride channel. *Nature* **375:**599–603

Franciolini, F., Nonner, W. 1994. Anion-cation interactions in the pore of neuronal background chloride channels. *J. Gen. Physiol.* **104:**711–723

Garber, S.S., Cahalan, M.D. 1997. Volume-regulated anion channels and control of a sample cell behavior. *Cell Physiol. Biochem.* **7:**229–241

Garber, S.S., Hoshi, T., Aldrich, R.W. 1989. Regulation of ionic currents in PC12 cells by NGF and dexamethasone. *J. Neurosci.* **9:**3976–3987

Hamill, O.P., Marty, A., Neher, E., Sakmann, B., Sigworth, F.J. 1981. Improved patch-clamp techniques for high-resolution current recording from cells and cell-free membrane patches. *Pfluegers Arch.* **391:**85–100

Hille, B. 1992. Ionic Channels of Excitable Membranes. Sinauer Associates Inc., Sunderland, MA

Huang, P., Liu, J., Di, A., Robinson, N.C., Musch, M.W., Kaetzel, M.A., Nelson, D.J. 2001. Regulation of human CLC-3 channels by multifunctional Ca^{2+}/calmodulin-dependent protein kinase. *J. Biol. Chem.* **276:**20093–20100

Hume, J.R., Duan, D., Collier, M.L., Yamazaki, J., Horowitz, B. 2000. Anion transport in heart. *Physiol. Rev.* **80:**31–81

Hussy, N., Deleuze, C., Desarmenien, M.G., Moos, F.C. 2000. Osmotic regulation of neuronal activity: a new role for taurine and glial cells in a hypothalamic neuroendocrine structure. *Prog. Neurobiol.* **62:**113–134

Huxtable, R.J. 1992. Physiological actions of taurine. *Physiol. Rev.* **72:**101–163

Jackson, P.S., Churchwell, K., Ballatori, N., Boyer, J.L., Strange, K. 1996. Swelling-activated anion conductance in skate hepatocytes: regulation by cell Cl^- and ATP. *Am. J. Physiol.* 270:C57–C66

Jackson, P.S., Strange, K. 1993. Volume-sensitive anion channels mediate swelling activated inositol and taurine efflux. *Am. J. Physiol.* **265:**C1489–C1500

Jackson, P.S., Strange, K. 1995. Characterization of the voltage-dependent properties of a volume-sensitive anion conductance. *J. Gen. Physiol.* **105:**661–671

Jentsch, T.J., Stein, V., Weinreich, F., Zdebik, A.A. 2002. Molecular structure and physiological function of chloride channels. *Physiol. Rev.* **82:**503–568

Lang, F., Busch, G.L., Ritter, M., Volkl, H., Waldegger, S., Gulbins, E., Haussinger, D. 1998a. Functional significance of cell volume regulatory mechanisms. *Physiol. Rev.* **78:**247–306

Lang, F., Lepple-Wienhues, A., Paulmichl, M., Szabo, I., Siemen, D., Gulbins, E. 1998b. Ion channels, cell volume, and apoptotic cell death. *Cell Physiol. Biochem.* **8:**285–292

Lang, F., Paulmichl, M. 1995. Properties and regulation of ion channels in MDCK cells. *Kidney Int.* **48:**1200–1205

Law, R.O. 1991. Amino acids as volume-regulatory osmolytes in mammalian cells. *Comp. Biochem. Physiol.* **99A:**263–277

Levitan, I., Garber, S.S. 1997. Volume regulated anion current and cytoskeletal interaction. *In*: From Ion Channels to Cell-Cell Conversations. Latorre R. and Sáez J.C., editors. pp. 245–267. Plenum Press, New York

Levitan, I., Garber, S.S. 1998. Anion competition for a volume-regulated current. *Biophys. J.* **75:**226–235

Lewis, R.S., Ross, P.E., Cahalan, M.D. 1993. Chloride channels activated by osmotic stress in T lymphocytes. *J. Gen. Physiol.* **101:**801–826

Li, X., Weinman, S.A. 2002. Chloride channels and hepatocellular function: prospects for molecular identification. *Annu. Rev. Physiol.* **64:**609–633

Lin, C.L., Tzingounis, A.V., Jin, L., Furuta, A., Kavanaugh, M.P., Rothstein, J.D. 1998. Molecular cloning and expression of the rat EAAT4 glutamate transporter subtype. *Brain Res. Mol. Brain Res.* **63:**174–179

Linsdell, P., Tabcharani, J.A., Hanrahan, J.W. 1997. Multi-ion mechanism for ion permeation and block in the cystic fibrosis transmembrane conductance regulator chloride channel. *J. Gen. Physiol.* **110:**365–377

Maduke, M., Miller, C., Mindell, J.A. 2000. A decade of CLC chloride channels: structure, mechanism, and many unsettled questions. *Annu. Rev. Biophys. Biomol. Struct.* **29:**411–438

Margolskee, R.F., McHendry-Rinde, B., Horn, R. 1993. Panning transfected cells for electrophysiological studies. *Biotechniques* **15:**906–911

McManus, M.L., Churchwell, K.B., Strange, K. 1995. Regulation of cell volume in health and disease. *New Eng. Med.* **333:**1260–1266

Nilius, B., Eggermont, J., Droogmans, G. 2000. The endothelial volume-regulated anion channel, VRAC. *Cell Physiol. Biochem.* **10:**313–320

Nilius, B., Eggermont, J., Voets, T., Buyse, G., Manolopoulos, V., Droogmans, G. 1997. Properties of volume-regulated anion channels in mammalian cells. *Prog. Biophys. Mol. Biol.* **68:**69–119

Nilius, B., Prenen, J., Voets, T., Eggermont, J., Droogmans, G. 1998. Activation of volume-regulated chloride currents by reduction of intracellular ionic strength in bovine endothelial cells. *J. Physiol.* **506:**353–361

Pasantes-Morales, H., Franco, R., Torres-Marquez, M.E., Hernandez-Fonseca, K., Ortega, A. 2000. Amino acid osmolytes in regulatory volume decrease and isovolumetric regulation in brain cells: contribution and mechanisms. *Cell Physiol. Biochem.* **10:**361–370

Qu, Z., Hartzell, H.C. 2000. Anion permeation in Ca^{2+}-activated Cl^- channels. *J. Gen. Physiol.* **116:**825–844

Reddy, M.M., Quinton, P.M. 2003. Control of dynamic CFTR selectivity by glutamate and ATP in epithelial cells. *Nature* **423:**756–760

Ross, P.R., Garber, S.S., Cahalan, M.C. 1994. Membrane chloride conductance and capacitance in Jurkat T lymphocytes during osmotic swelling. *Biophys. J.* **66:**169–178

Sabirov, R.Z., Prenen, J., Tomita, T., Droogmans, G., Nilius, B. 2000. Reduction of ionic strength activates single volume-regulated anion channels (VRAC) in endothelial cells. *Pfluegers Arch.* **439:**315–320

Smith, G.L., Miller, D.J. 1985. Potentiometric measurements of stoichiometric and apparent affinity constants of EGTA for protons and divalent ions including calcium. *Biochim. Biophys. Acta* **839:**287–299

Song, D., O'Regan, M.H., Phillis, J.W. 1998. Amino acid release during volume regulation by cardiac cells: cellular mechanisms. *Eur. J. Pharmacol.* **341:**273–280

Stutzin, A., Eguiguren, A.L., Cid, L.P., Sepulveda, F.V. 1997. Modulation by extracellular Cl^- of volume-activated organic osmolyte and halide permeabilities in HeLa cells. *Am. J. Physiol.* **273:**C999–C1007

Stutzin, A., Eguiguren, A.L., Montes, N., Sepulveda, F.V. 1998. Modulation by extracellular and intracellular iodide of volume-activated Cl^- current in HeLa cells. *Pfluegers Arch.* **436:**152–154

Stutzin, A., Torres, R., Oporto, M., Pacheco, P., Eguiguren, A.L., Cid, L.P., Sepulveda, F.V. 1999. Separate taurine and chloride efflux pathways activated during regulatory volume decrease. *Am. J. Physiol.* **277:**C392–C402

Voets, T., Droogmans, G., Raskin, G., Eggermont, J., Nilius, B. 1999. Reduced intracellular ionic strength as the initial trigger for activation of endothelial volume-regulated anion channels. *Proc. Natl. Acad. Sci. USA* **96:**5298–5303

Zipfel, G.J., Babcock, D.J., Lee, J.M., Choi, D.W. 2000. Neuronal apoptosis after CNS injury: the roles of glutamate and calcium. *J. Neurotrauma* **17:**857–869